CANCER BIOTHERAPY AND RADIOPHARMACEUTICALS
Volume 32, Number 2, 2017

DOI: 10.1089/cbr.2016.2141

A Radiolabeled Fully Human Antibody to Human Aspartyl (Asparaginyl) β-Hydroxylase Is a Promising Agent for Imaging and Therapy of Metastatic Breast Cancer

Ekaterina Revskaya,[1] Zewei Jiang,[1] Alfred Morgenstern,[2] Frank Bruchertseifer,[2] Muctarr Sesay,[3] Susan Walker,[4] Steven Fuller,[4] Michael S. Lebowitz,[4] Claudia Gravekamp,[1] Hossein A. Ghanbari,[4] and Ekaterina Dadachova[1]

Abstract

There is a need for novel effective and safe therapies for metastatic breast cancer based on targeting tumor-specific molecular markers of cancer. Human aspartyl (asparaginyl) β-hydroxylase (HAAH) is a highly conserved enzyme that hydroxylates epidermal growth factor-like domains in transformation-associated proteins and is overexpressed in a variety of cancers, including breast cancer. A fully human monoclonal antibody (mAb) PAN-622 has been developed to HAAH. In this study, they describe the development of PAN-622 mAb as an agent for imaging and radioimmunotherapy of metastatic breast cancer. PAN-622 was conjugated to several ligands such as DOTA, CHXA″, and DTPA to enable subsequent radiolabeling and its immunoreactivity was evaluated by an HAAH-specific enzyme-linked immunosorbent assay and binding to the HAAH-positive cells. As a result, DTPA-PAN-622 was chosen to investigate biodistribution in healthy CD-1 female mice and 4T1 mammary tumor-bearing BALB/c mice. The ^{111}In-DTPA-pan622 mAb concentrated in the primary tumors and to some degree in lung metastases as shown by SPECT/CT and Cherenkov imaging. A pilot therapy study with ^{213}Bi—DTPA-PAN-622 demonstrated a significant effect on the primary tumor. The authors concluded that human mAb PAN-622 to HAAH is a promising reagent for development of imaging and possible therapeutic agents for the treatment of metastatic breast cancer.

Keywords: ^{111}In, ^{213}Bi, HAAH, metastatic breast cancer, PAN-622 human antibody, radioimmunotherapy

Introduction

Human aspartyl (asparaginyl) β-hydroxylase (HAAH) is a highly conserved enzyme that hydroxylates epidermal growth factor-like domains in transformation-associated proteins. Overexpression of this enzyme has been detected in a variety of cancers, including breast cancer.[1–5] In contrast, the expression of HAAH in normal tissue is low and the protein is generally localized only to internal compartments (e.g., endoplasmic reticulum). It has been demonstrated that on cellular transformation, HAAH is overexpressed and translocated to the tumor cell surface, rendering it a specific surface antigen for tumor cells.

Although significant progress has been made in recent decades in treatment of metastatic breast cancer,[6] it still remains a formidable threat occupying third place in the list of cancers killing the highest number of American women and men (American Cancer Society data). Thus, there is a need for novel effective and safe therapies for metastatic breast cancer based on targeting tumor-specific molecular markers of cancer.[7] Radioimmunotherapy (RIT) involves selective targeting of radionuclides to cancer-associated cell surface antigens using monoclonal antibodies (mAbs). RIT permits the delivery of a high dose of therapeutic radiation to cancer cells, while minimizing the exposure of normal cells. Although this approach has been investigated for several decades, the cumulative advances in cancer biology, antibody engineering, and radiochemistry in the past decade have markedly enhanced the ability of RIT to produce durable remissions of multiple cancer types.[8]

The authors have produced a fully human IgG, PAN-622, which specifically targets HAAH on the surface of cancer

[1]Department of Radiology, Albert Einstein College of Medicine, Bronx, New York.
[2]European Commission, Joint Research Centre, Directorate for Nuclear Safety and Security, Karlsruhe, Germany.
[3]Goodwin Biotechnology, Plantation, Florida.
[4]Panacea Pharmaceuticals, Gaithersburg, Maryland.

Address correspondence to: Hossein A. Ghanbari; Panacea Pharmaceuticals, Inc.; 209 Perry Parkway, Suite 13, Gaithersburg, MD 20877
E-mail: **hag@panaceapharma.com**

cells.[3] Furthermore, the antibody has been shown to internalize into tumor cells and serve as a vehicle for the delivery of cytotoxic moieties.[3] In this study, the authors describe the development of the PAN-622 mAb as an agent for imaging and RIT of metastatic breast cancer.

Materials and Methods

Conjugation of PAN-622 to various ligands to enable radiolabeling

PAN-622 and its conjugates were produced by Goodwin Biotechnology (Plantation, FL). To enable radiolabeling of PAN-622 with diagnostic and therapeutic radionuclides, it was conjugated to NHS-DOTA and maleimide-DOTA, bifunctional CHXA″, and maleimide-DTPA. Two conjugation procedures were performed as follows:

(1) Random Conjugation: The purified PAN-622 antibody (5 mg/mL) was concentrated and diafiltered into the conjugation buffer (50 mM sodium carbonate, 150 mM sodium chloride, 5 mM EDTA, pH 8.6) using Amicon Ultra 50 kDa MWCO filters. The buffer exchanged PAN-622 antibody was divided into three aliquots for each of the three conjugation reactions. Each PAN-622 aliquot was reacted with CHXA″-DTPA solubilized into 50 mM sodium carbonate, 150 mM sodium chloride, 5 mM EDTA, pH 8.6, at 2:1, 5:1, and 10:1 mole ratios of CHXA″-DTPA to PAN-622 antibody. The reaction mixtures were incubated at 25°C overnight (16 hours). The conjugation reaction was quenched with 1 M Tris, pH 8.6, by incubating the reaction mixtures for an additional 1 hour at 25°C. The three CHXA″-DTPA-PAN-622 conjugates were purified and buffer exchanged into the 150 mm ammonium acetate buffer, pH 6.5, using a Pellicon XL Biomax 50 kDa TFF membrane.

(2) Site-Directed Conjugation: The purified PAN-622 antibody (5 mg/mL) was diafiltered in Dulbecco's phosphate-buffered saline (PBS), pH 6.7, containing 5 mM EDTA. Partial reduction of one of the two hinge disulfide bonds was achieved by addition of TCEP as the reducing reagent. The diafiltered pan622 antibody was split into three aliquots. TCEP was added at a 10:1 mole ratio of TCEP to PAN-622 and each sample was incubated at 25°C for 8, 15, and 30 minutes. Following the incubations, each reaction mixture was reacted with DOTA-MAL (maleimide) or DTPA-MAL (in DPBS, 5 mM EDTA, pH 6.7) at a 50:1 mole ratio DOTA-MAL or DTPA-MAL: PAN-622 at 25°C for 2 hours. After conjugation, each reaction mixture was quenched with NEM (in DPBS, 5 mM EDTA, pH 6.7, at a 2:1 mole ratio of DOTA-MAL or DTPA-MAL:NEM and incubated for 30 minutes at 25°C. The DOTA-MAL-PAN-622 and DTPA-MAL-PAN-622 conjugates were purified and buffer exchanged into the ammonium acetate buffer as above.

Immunoreactivity determination

The immunoreactivity of the resulting conjugates toward HAAH was assessed by an enzyme-linked immunosorbent assay (ELISA) and binding to HAAH-expressing lung cancer cells. In the standard ELISA, high protein binding plates were coated with a recombinant form of HAAH corresponding to the catalytic domain of the protein. Wells were coated at 5 μg/mL protein in 0.1 M phosphate buffer, pH 7.4, blocked with 1% nonfat dry milk, and then incubated with conjugated PAN-622 at varying concentrations. The secondary antibody was goat antihuman IgG-γ-HRP (1 μg/mL, KPL, cat# 074-1002) and plates were developed with TMB. For the cell binding assay, H460 (human lung cancer) or 4T1 (mouse breast cancer) cells were grown in 96-well plates and fixed with 0.25% fixative glutaraldehyde (Sigma). This served as the coating step, and the remainder of the assay was performed as in the standard ELISA.

Radiolabeling of ligand-conjugated PAN-622

^{111}In was procured from Nordion. ^{213}Bi was eluted from a ^{225}Ac/^{213}Bi generator provided by the European Commission, Karlsruhe, Germany.[9] For radiolabeling of the conjugates with ^{111}In, 100 μg of each conjugate in ammonium acetate buffer, pH 5.5, was placed in a 0.5 mL low protein binding Eppendorf tube. Two microliters of ^{111}In solution (200 μCi) in 0.15 M ammonium acetate buffer, pH 5.5, was added to each tube, thus making the specific activity of radiolabeled protein 2 μCi/μg. The samples were incubated for 30 minutes at 37°C in an orbital thermomixer at 1000 rpm. At the end of the incubation period, the reaction was quenched with the addition of 3 μL 0.05 M EDTA and the radiolabeling yields were assessed as below. For radiolabeling with ^{213}Bi, the ^{225}Ac/^{213}Bi generator was eluted with 500 μL of 0.1 M HI. The eluant contained 150–1500 μCi ^{213}Bi. The pH of the eluant was adjusted to $\sim$5.0 by adding 80 μL of 2.5 M ammonium acetate buffer. This ^{213}Bi-containing solution was added to the tube with 100 μg DTPA-PAN-622 mAb, and the reaction mixture was incubated for 6 minutes at 37°C. At the end of the incubation period, the reaction was quenched by the addition of 3 μL 0.05 M EDTA, and the radiolabeling yield was assessed.

The radiolabeling yields were measured by instant thin layer chromatography. The 10 cm silica gel was spotted with 1 μL of radiolabeled antibody and developed in 0.15 M ammonium acetate buffer, pH 5.5. The strips were subsequently cut in half and counted in a γ counter. The measurements were performed in triplicate. The radiolabeling yields were calculated as $(R/(R+F)) \times 100\%$, where R (radiolabeled) are the counts in the lower half of the strip where the radiolabeled antibody is localized and F (free) are the counts in the upper part of the strip where the free ^{111}In in the form of an EDTA complex is localized. The radiolabeled antibodies were subsequently analyzed by radio-high performance liquid chromatography (HPLC). A Waters HPLC system equipped with a Bioscan flow-through radiation detector was used. The size exclusion TSK3000XL column was eluted with PBS, pH 7.4, at 1 mL/min.

Cell binding and cell internalization studies

5×10^5–2×10^6 4T1 mouse mammary cancer cells (CRL-2539; ATCC) were placed in 1 mL PBS in the Eppendorf tubes preblocked with 1% BSA to prevent binding of the radiolabeled antibody to the tubes. Each sample was prepared in triplicate. The ^{111}In-DTPA-PAN-622 antibody in the amount of 12 ng per sample was added to the cells and the tubes were incubated for 1 hour at 37°C, followed by

Table 1. Radiolabeling Yields with ^{111}In for CHXA″- and DOTA-Conjugated PAN-622 Monoclonal Antibody

Conjugate	*Radiolabeling yield, %*
CHXA″-PAN-622, 2 molar ratio	11.7 ± 0.5
CHXA″-PAN-622, 10 molar ratio	17.0 ± 1.2
CHXA″-PAN-622, 20 molar ratio	61.1 ± 2.1
CHXA″-PAN-622, 50 molar ratio	3.0 ± 0.2
DOTA-PAN-622-MAL, 8 minutes	0.07 ± 0.01
DOTA-PAN-622-MAL, 15 minutes	0.07 ± 0.01
DOTA-PAN-622-MAL, 30 minutes	0.10 ± 0.02
DOTA-PAN-622-NHS, 10:1	0.05 ± 0.01
DOTA-PAN-622-NHS, 20:1	0.19 ± 0.02

counting the tubes in the γ counter, spinning down the cell pellet, removing the supernatant, washing the pellet with 2×1 mL cold PBS, and counting the cell pellets in the γ counter. To ascertain the specificity of ^{111}In-DTPA-PAN-622 binding to HAAH on 4T1 cells, the authors used the ^{111}In-labeled isotope matching control mAb 2556, which is a fully human mAb to HIV-1 gp41 glycoprotein.[10] As an additional control, they used 4T1 cells preincubated for 1 hour with 10 μg/mL PAN-622.

The internalization of ^{111}In-DTPA-PAN-622 into the 4T1 cells was investigated using the methodology described in Ref.[11] Briefly, the 4T1 cells were incubated with ^{111}In-DTPA-PAN-622 at 4°C for 1 hour to obtain surface labeling with minimal internalization. Aliquots of 10^6 cells were then placed into separate tubes and supernatants were separated from cells. Immediately after separation, cells underwent acid wash and acid-resistant radioactivity was determined by counting cell pellets after centrifugation. This procedure was repeated at various times after transferring cell aliquots to an incubator at 37°C. Acid-resistant fraction was determined by dividing activity in cell pellet after acid wash by total activity on cell after 1 hour of incubation at 4°C.

Biodistribution of ^{111}In-PAN-622 in healthy mice

All animal experiments were performed according to the protocol approved by the Institute for Animal Studies at the

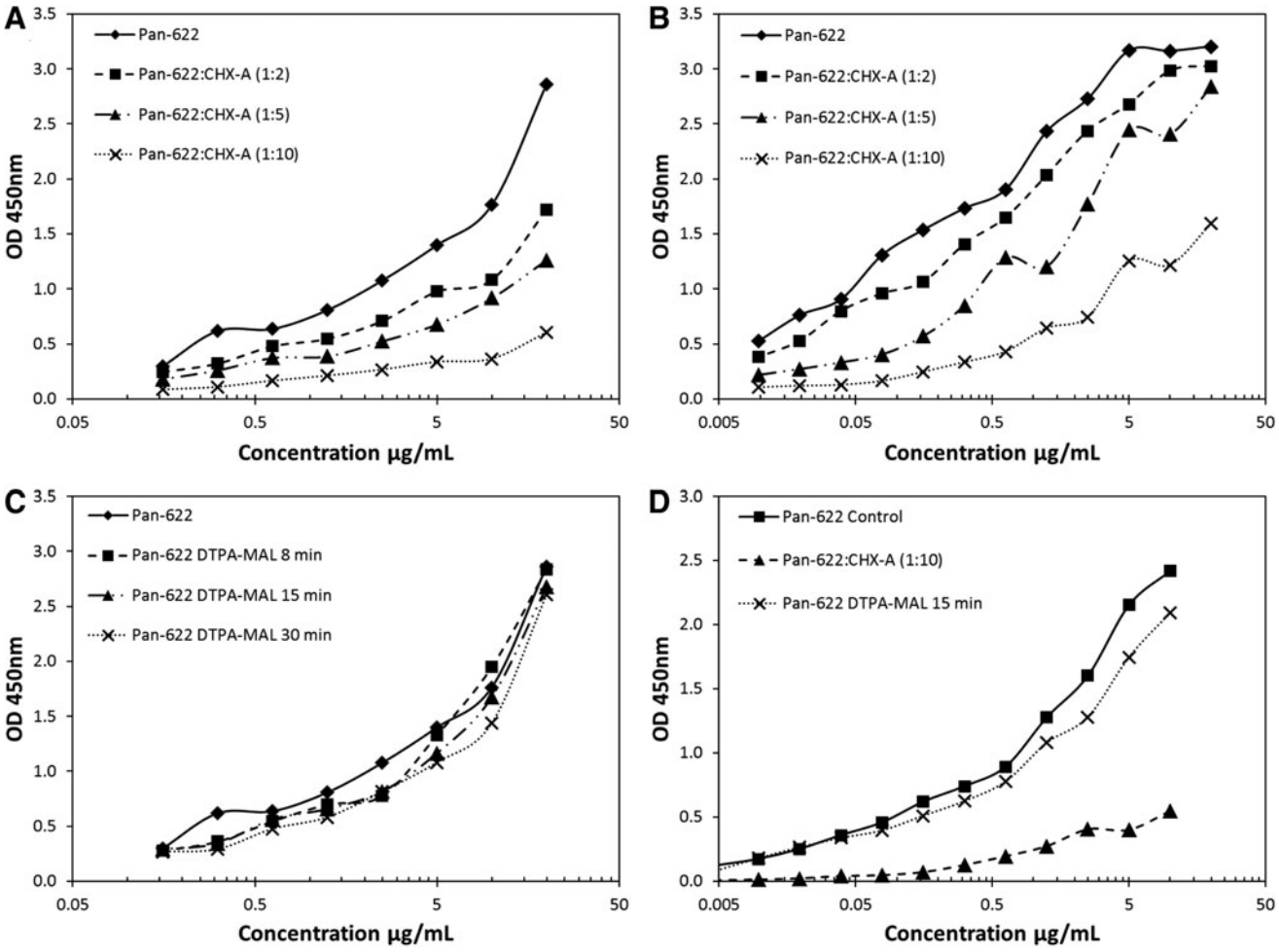

FIG. 1. Binding of PAN-622 conjugates to HAAH and cancer cells. **(A)** Binding of PAN-622-CHXA'' conjugates to recombinant HAAH catalytic domain by ELISA; **(B)** binding of PAN-622-CHXA'' conjugates to H460, human lung cancer cells as measured by cellular ELISA; **(C)** binding of PAN-622-DTPA-MAL conjugates to recombinant HAAH catalytic domain by ELISA; **(D)** binding of PAN-622-DTPA-MAL, 15 minutes, and PAN-622-CHXA'' 10:1 conjugates to 4T1, mouse breast cancer cells as measured by cellular ELISA. mAU, milli absorbance units. ELISA, enzyme-linked immunosorbent assay; HAAH, human aspartyl (asparaginyl) β-hydroxylase.

Table 2. Radiolabeling Yields with ^{111}In for DTPA-Conjugated PAN-622 Monoclonal Antibody

Conjugate	*Radiolabeling yield, %*
PAN-622 DTPA-mal 8 minutes	12.53 ± 1.02
PAN-622 DTPA-mal 15 minutes	93.78 ± 0.79
PAN-622 DTPA-mal 30 minutes	93.12 ± 0.98

Albert Einstein College of Medicine. Twenty-five healthy (i.e., naive) CD-1 female mice were injected with an intraperitoneal (IP) dose of ^{111}In-DTPA-PAN-622 antibody (0.020 mg and 50 μCi per mouse). Mice were euthanized at 1, 12, 24, 48, and 96 hours subsequent to dosing ($n = 5$ mice per time point). Tissue samples (brain, muscle, bone, heart, lung, liver, spleen, kidneys, stomach, large intestine, blood, and urine) were collected from each mouse, weighed, and the accumulated activity per tissue counted in a γ counter.

Biodistribution of ^{111}In-DTPA-PAN-622 and Cherenkov imaging in 4T1 mammary tumor-bearing mice

Twenty-five 6–8-week-old female BALB/c mice were injected with 10^5 4T1 mammary cancer cells into the mammary fat pad. The primary tumors formed in the mammary fat pad and became palpable on Day 10 postcell injection. The authors have previously demonstrated histologically that in this model, lung metastases start to appear on approximately Day 14 postcell injection.[12] The tumor-bearing mice were given ^{111}In-DTPA-PAN-622 on Day 18 postcell injection. Twenty-two of the 4T1 tumor-bearing mice were injected with an IP dose of ^{111}In-DTPA-PAN-622 antibody (0.020 mg and 50 μCi per mouse). Mice were euthanized at 1, 12, 24, 48, and 96 hours ($n = 4$–5 mice per time point). Tumors and tissue samples (brain, muscle, bone, heart, lungs, liver, spleen, kidneys, stomach, large intestine, blood, and eyes for 48- and 96-hour time points) were collected from each mouse, weighed, and the accumulated activity per tissue counted in a γ counter.

For Cherenkov imaging, three 4T1 tumor-bearing mice were injected with an IP dose of ^{111}In-DTPA-PAN-622 antibody (0.030 mg and 200 μCi per mouse). The mice were imaged at 24 and 48 hours post ^{111}In-DTPA-PAN-622 antibody in supine and prone positions on IVIS Spectrum Imaging System (PerkinElmer, Waltham, MA) in luminescence mode with 20 minutes of exposure while being anesthetized with isoflurane from a built-in source. Living Image Version 4.3.1.0.15880 software was used to generate the images.

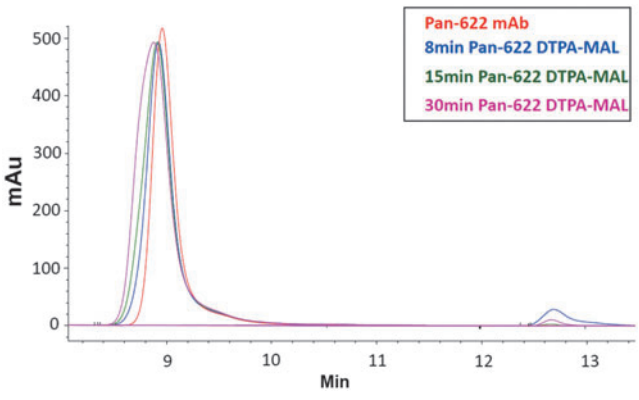

FIG. 2. Structural evaluation of Pan622 conjugates: HPLC-SEC overlay of PAN-622 DTPA-MAL conjugates along with naked PAN-622 mAb. mAb, monoclonal antibody.

Pilot therapy of 4T1 tumor-bearing mice with ^{213}Bi-DTPA-PAN-622 and microSPECT/CT imaging with ^{111}In-DTPA-PAN-622

Eight 6–8-week-old female BALB/c mice were injected with 10^5 4T1 cells into the mammary fat pad. The primary tumors in the mammary fat pad became palpable in all mice on Day 10 postcell injection. Four mice were treated on Days 5 and 8 postcell injection with 150 μCi ^{213}Bi-PAN-622 via IP injection, whereas the other four mice were left untreated. On Day 21 postcell injection, all tumor-bearing mice were given 200 μCi ^{111}In-DTPA-PAN-622 via IP injection and imaged at 4, 24, and 48 hours after administration with microSPECT/CT. One week after the last imaging time point, the mice were sacrificed, their primary tumors removed and weighed, and their lungs were perfused with India ink and the metastases quantified.

Results

Attachment of DTPA to PAN-622 via maleimide conjugation enabled radiolabeling and preserved PAN-622 immunoreactivity

The authors initially investigated the suitability of random attachment of the bifunctional CHXA″-DTPA chelator to the PAN-622 antibody for subsequent radiolabeling with ^{111}In. The nonreducing sodium dodecyl sulfate/polyacrylamide gel electrophoresis (SDS-PAGE) showed some attachment of CHXA″-DTPA to PAN-622 (Supplementary Fig. S1A; Supplementary Data are available online at www.liebertpub.com/cbr). Conjugation of PAN-622 with a 2- to 20-fold molar excess of CHXA"-DTPA resulted in increasing levels of radiolabeling from 11.7% to 61.1%, however, at a 50-fold molar excess, radiolabeling yield dropped precipitously to 3.0% (Table 1). Unfortunately, increased levels of conjugation with CHXA" also resulted in a loss of binding capacity to both recombinant HAAH protein and to tumor cells (Fig. 1A, B). Next, both the site-specific conjugation via DOTA-MAL and random conjugation via NHS-DOTA of the macrocyclic chelator DOTA to PAN-622 were attempted. No radiolabeling of resulting conjugates with ^{111}In was observed, pointing to possible incompatibility of a large macrocycle molecule with PAN-622 (Table 1). In the final attempt, site-specific conjugation of DTPA-MAL chelator to the PAN-622 mAb was done. DTPA-MAL chelator was attached to PAN-622 using 8, 15, and 30 minutes of reaction times. The resulting conjugates after 15- or 30-minute reactions were labeled with ^{111}In with a 93% efficiency (Table 2). These conjugates showed structural intactness by size exclusion HPLC (Fig. 2) and nonreducing SDS-PAGE (Supplementary Fig. S1B) and preserved their immunoreactivity toward HAAH as per ELISA and cell binding (Fig. 1C, D). In all subsequent *in vivo* experiments, the 15-minute maleimide DTPA-PAN-622 conjugate was used.

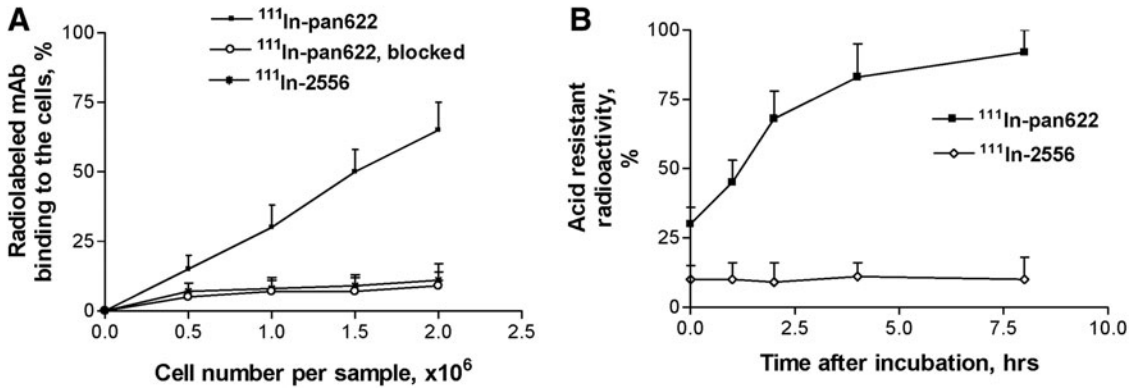

FIG. 3. Binding and internalization of ^{111}In-DTPA-pan622 antibody in 4T1 cells: **(A)** binding of ^{111}In-DTPA-pan622 antibody to 4T1 cells. For control, 4T1 cells were preblocked with cold PAN-622. Another control was isotype-matching ^{111}In-DTPA-2556 antibody to HIV-1 gp41; **(B)** internalization of ^{111}In-DTPA-PAN-622 antibody into 4T1 cells. The percentage of radioactivity remaining in the cells after the acid wash is shown.

Binding of ^{111}In-DTPA-PAN-622 to 4T1 cells was HAAH specific and resulted in its internalization

The binding of ^{111}In-DTPA-PAN-622 to 4T1 cells is shown in Figure 3A. The absence of ^{111}In-DTPA-PAN-622 binding to the cells preblocked with the excess of cold pan622, and practically no binding of the isotype matching control mAb ^{111}In-DTPA-2556 to the cells proved that the binding of ^{111}In-DTPA-PAN-622 to 4T1 cells was HAAH specific. This binding resulted in the robust internalization of ^{111}In-DTPA-PAN-622 into the cells (Fig. 3B), which was completed by 8 hours. No internalization of the control mAb ^{111}In-DTPA-2556 into the cells was observed (Fig. 3B).

Biodistribution of ^{111}In-DTPA-PAN-622 in healthy mice demonstrated its overall stability and fast clearance from major organs

Figure 4 shows the results of the biodistribution of ^{111}In-DTPA-PAN-622 in healthy female CD-1 mice. The radiolabeled conjugate cleared rapidly from the circulation with less than 1% ID/gram remaining in the blood at 96 hours postinjection. The clearance from the blood-rich organs such as the heart and lungs followed the same trend. The processing and excretion of the ^{111}In-DTPA-PAN-622 conjugate followed the hepatobiliary route, which is typical for the conjugates labeled with a trivalent residualizing radiometal such as ^{111}In. This *in vivo* stability of ^{111}In-DTPA-PAN-622 provided the impetus for the follow-up experiments in mammary tumor-bearing mice.

^{111}In-DTPA-PAN-622 concentrated in 4T1 mammary tumors in balb/c mice

The follow-up biodistribution study of ^{111}In-DTPA-PAN-622 in 4T1 tumor-bearing female BALB/c mice confirmed the fast clearance of the radiolabeled conjugate from the circulation and demonstrated its specific uptake in 4T1 primary tumors and elevated uptake in the lung metastases (Fig. 5). The tumor and lung uptake of ^{111}In-DTPA-PAN-622 was also observed on Cherenkov luminescence images (Fig. 6). To the best of knowledge, these are the first reported *in vivo* images of Cherenkov luminescence from ^{111}In, which besides γ rays also emits Auger electrons. It is important to note here that Cherenkov luminescence *in vivo*

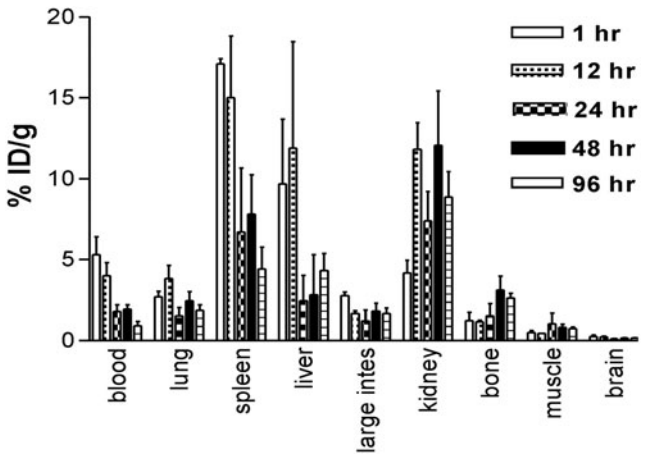

FIG. 4. Biodistribution of ^{111}In-DTPA-PAN-622 antibody in healthy CD-1 mice.

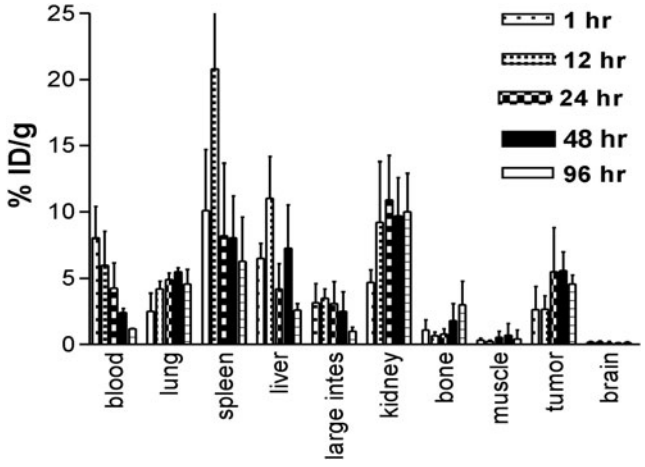

FIG. 5. Biodistribution of ^{111}In-DTPA-PAN-622 antibody in 4T1 tumor-bearing mice.

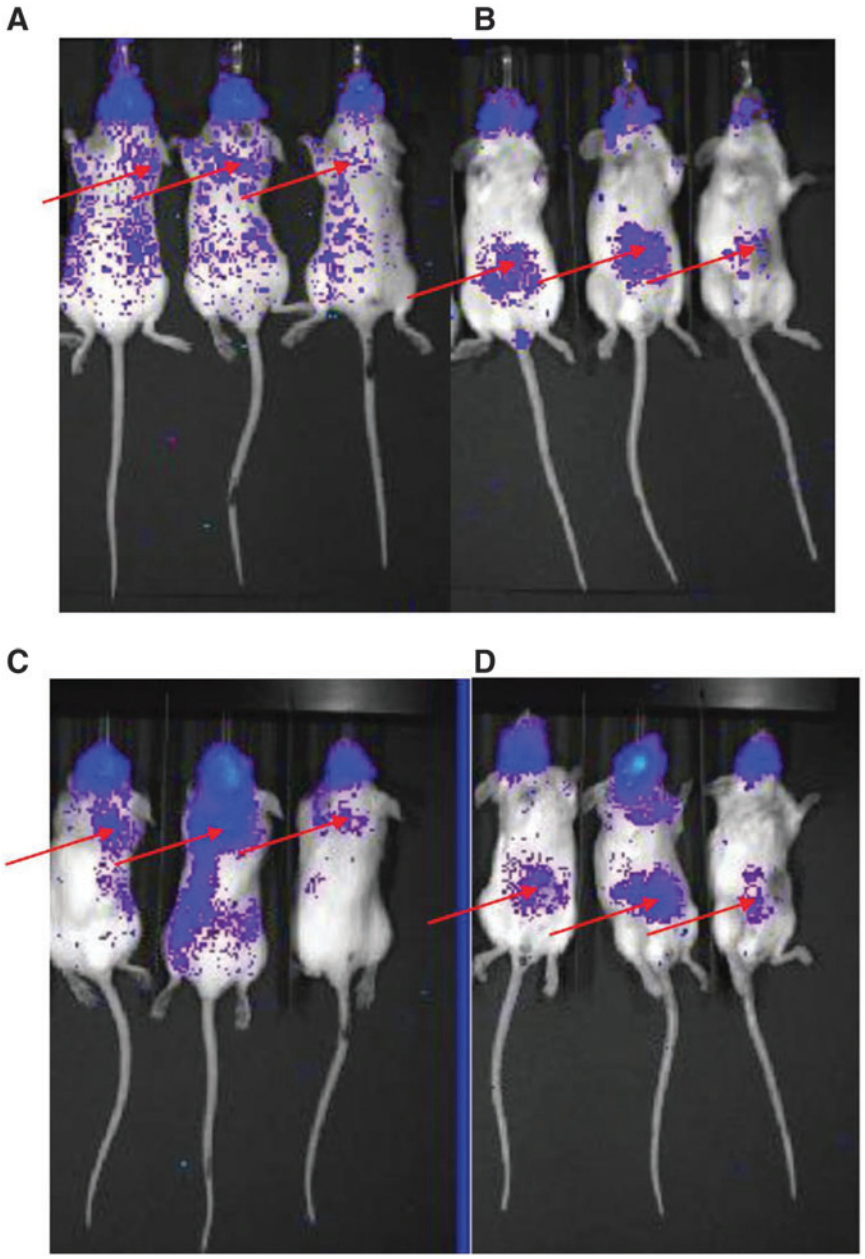

FIG. 6. 4T1 tumor-bearing balb/c mice injected with ^{111}In-DTPA-PAN-622 antibody and imaged on IVIS Imager for Cherenkov luminescence at 24 and 48 hours postinjection: **(A)** 24 hours, mice in prone position; **(B)** 24 hours, mice in supine position; **(C)** 48 hours, mice in prone position; **(D)** 48 hours, mice in supine position. The suggested location of the lung metastases **(A, C)** and primary tumors in the mammary fat pad **(B, D)** is shown with *red arrows*.

is not a quantitative technique as the intensity of emitted light depends on the depth in the body and can only complement conventional biodistribution.

Treatment of 4T1 tumor-bearing mice with ^{213}Bi-PAN-622 reduced the size of primary tumors but not the number of the lung metastases

In this pilot therapy study with ^{213}Bi-DTPA-PAN-622, half of the 4T1 tumor-bearing mice were treated on Days 5 and 8 postcell injection with 150 μCi ^{213}Bi-PAN-622 via IP injection, while the other half of the mice were left untreated. On Day 21 postcell injection, all tumor-bearing mice were given IP injection of 200 μCi of ^{111}In-DTPA-PAN-622 and imaged at 4, 24, and 48 hours after its administration with microSPECT/CT. At all time points, there was significant uptake of ^{111}In-DTPA-PAN-622 in the peritoneum of the untreated mice which was practically absent in the ^{213}Bi-DTPA-PAN-622-treated mice (Fig. 7). This can be explained by the micrometastatic spread of the tumor cells in the peritoneum. In treated mice, the majority of activity was concentrated in the liver where the antibody is metabolized.

There was some diffuse uptake of ^{111}In-DTPA-PAN-622 in the lungs of the untreated mice, and no visible uptake in the lungs of ^{213}Bi-DTPA-PAN-622-treated mice. The pathological investigation revealed that the weight of the primary tumors was significantly ($p = 0.04$) less in ^{213}Bi-DTPA-PAN-622-treated mice than in untreated (Fig. 8A). The number of metastases in the lungs of both groups was practically the same ($p = 0.08$) (Fig. 8B).

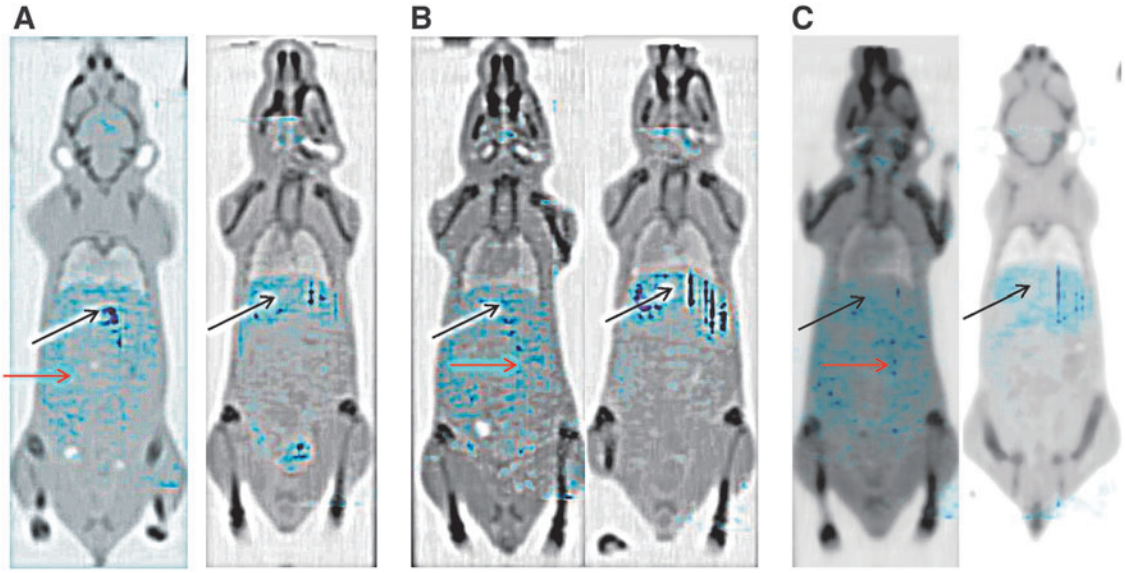

FIG. 7. microSPECT/CT with ^{111}In-DTPA-PAN-622 of 4T1 tumor-bearing mice: **(A)** 4 hours postinjection of ^{111}In-DTPA-PAN-622; **(B)** 24 hours; **(C)** 48 hours (*left panel* untreated mice; *right panel* treated with ^{213}Bi-DTPA-PAN-622). The *dark blue* color corresponds to the highest levels of radioactivity in the organs, the *light blue*—the lowest. *Black arrows* are pointing to the liver in all mice, *red arrows* are pointing to the peritoneal accumulation of radioactivity in untreated tumor-bearing mice.

Discussion

In this study, the authors investigated the utility of the radiolabeled fully human antibody, PAN-622, which targets HAAH for the *in vivo* imaging and therapy of metastatic breast cancer. HAAH has emerged as a promising biomarker of cancer cells.[1–5] HAAH is an oncofetal antigen that modulates *NOTCH* signaling pathways during embryogenesis.[13–16] In the adult mammal, HAAH expression is generally low and is localized to the intracellular compartments. Several studies have demonstrated that it is not significantly expressed on the surface of normal human tissues.[5,17] The protein is most highly expressed in the trophoblastic cells, where it is thought to play a role in uterine implantation.[13,16,18] PAN-622 has been previously developed as a fully human anti-HAAH antibody for use in immunotherapy of cancer without the radiolabel.[3] There was some uptake in the heads of all mice visible on Cherenkov and SPECT images but not confirmed by the biodistribution data. It has been demonstrated that HAAH is expressed in primitive neuroectodermal tumors but not in normal brain.[19] The authors would posit that as the 4T1 is a highly invasive and metastatic tumor, which is well established to metastasize to the brain[20,21]—the uptake in the head might be due to the metastases in the skull. It is unclear whether this observation is significant or not and thus warrants further investigation. The number of metastases in the lungs of both groups was practically the same; it might be possible that some of those

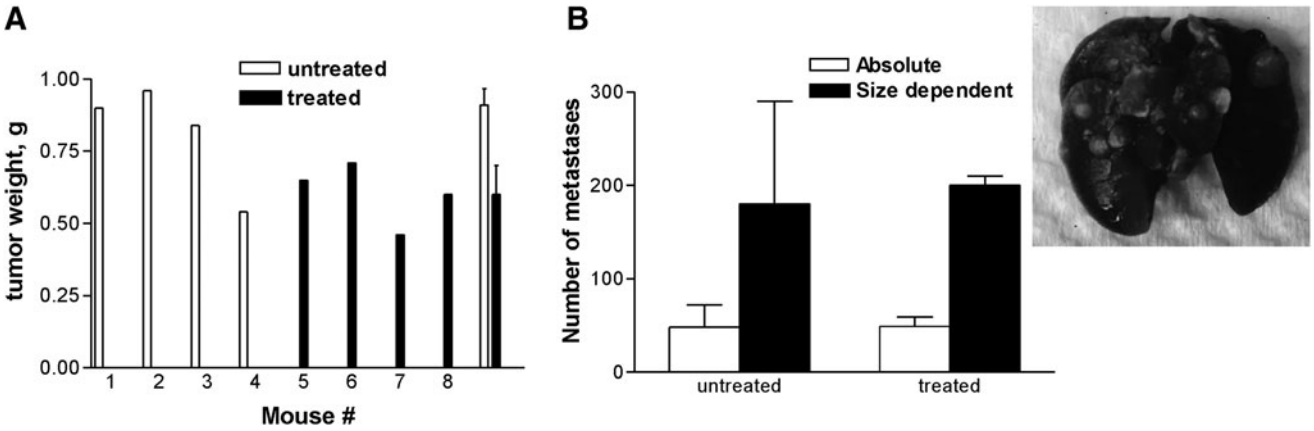

FIG. 8. Pathological examination of the 4T1 tumor-bearing mice treated with ^{213}Bi-DTPA-PAN-622: **(A)** the weights of the primary tumors from treated and untreated mice; **(B)** the number of metastases in the lungs of treated and untreated mice. The graph contains the insert with the image of metastases in the lungs perfused with India ink. The weight of the primary tumors was significantly ($p = 0.04$) less in ^{213}Bi-DTPA-PAN-622-treated mice than in untreated mice. The number of metastases in the lungs of both groups was practically the same ($p = 0.08$).

metastases in the ^{213}Bi-DTPA-PAN-622-treated group do not have any cells left expressing HAAH and for that reason there was no lung uptake on the microSPECT/CT images. Also, the 1-week lag between the last imaging session and opening of the mice might have contributed to the emergence of additional lung metastases.

Several radioimmunoimaging and RIT preclinical studies targeting other surface antigens such as HER-2 or EGFR in breast cancer with β-, α-, or Auger electron-emitting radionuclides are currently ongoing.[22–24] For the pilot therapy study in 4T1 tumor-bearing mice, the authors have selected an α-emitter ^{213}Bi. The use of targeted therapy with α-particle emitters in oncology is burgeoning worldwide. This is driven by the advantages of α-emitters over β-emitters, including very specific targeting of the diseased cells due to the α-particles' short 50–80 μm tissue range, and increased killing efficiency due to high linear energy transfer. This results in a controlled therapeutic modality with minimal normal tissue effects.[25] RIT with α-emitters does not depend on the oxygenation status of the tumor or its resistance to chemotherapy and external beam radiation therapy, as recently demonstrated by ^{213}Bi-labeled peptide-induced remission in patients with neuroendocrine tumors refractory to β-radiation.[26] In particular, ^{213}Bi-labeled mAbs have been used in multiple clinical trials for several oncologic indications and have demonstrated efficacy without major side-effects.[27,28] Likewise, the multiple administrations of ^{213}Bi-DTPA-PAN-622 in this study was well tolerated with treated animals showing no changes in their body conditioning scores. In contrast to this complete absence of toxicity, the researchers who used ^{225}Ac-labeled trastuzumab had to resort to intraductal administration of the radiolabeled antibody because of the high systemic toxicity of ^{225}Ac-trastuzumab.[22] Li et al. also utilized trastuzumab, which they labeled with Auger electron emitter ^{111}In to kill human breast cancer cells,[23] however, their results are so far only preliminary *in vitro* data, and it remains to be seen if ^{111}In will show promise in treating experimental breast cancer *in vivo*. The study, where the engineered immunoconjugates labeled with more traditional radionuclide ^{177}Lu and targeting both HER2 and EGFR on the surface of breast cancer xenografts in mice were used,[24] demonstrated comparable efficacy and lack of toxicity observed in this work.

In conclusion, these results demonstrated that radiolabeled human mAb PAN-622 to HAAH is a promising reagent for imaging and possible therapy of metastatic breast cancer. Further experiments in a mouse model of breast cancer with parallel use of two cell lines—one expressing HAAH and the other one not expressing HAAH, are currently being planned. Since HAAH is overexpressed in other cancers the use of radiolabeled PAN-622 will be explored in other cancers as well.

Acknowledgments

The study was performed under an academic/industrial research agreement funded by Panacea Pharmaceuticals, Inc., the European Commission (A.M. and F.B.) and the National Cancer Institute Grant 1 R21 CA199010-01 (C.G.).

Disclosure Statement

No competing financial interests exist.

References

1. Lavaissiere L, Jia S, Nishiyama M, et al. Overexpression of human aspartyl(asparaginyl)beta-hydroxylase in hepatocellular carcinoma and cholangiocarcinoma. J Clin Invest 1996;98:1313.
2. Ince N, de la Monte SM, Wands JR. Overexpression of human aspartyl (asparaginyl) beta-hydroxylase is associated with malignant transformation. Cancer Res 2000;60:1261.
3. Yeung YA, Finney AH, Koyrakh IA, et al. Isolation and characterization of human antibodies targeting human aspartyl (asparaginyl) beta-hydroxylase. Hum Antibodies 2007; 16:163 .
4. Xue T, Xue XP, Huang QS, et al. Monoclonal antibodies against human aspartyl (asparaginyl) beta-hydroxylase developed by DNA immunization. Hybridoma (Larchmt) 2009;28:251.
5. Yang H, Song K, Xue T, et al. The distribution and expression profiles of human Aspartyl/Asparaginyl beta-hydroxylase in tumor cell lines and human tissues. Oncol Rep 2010;24:1257.
6. Jin X, Mu P. Targeting breast cancer metastasis. Breast Cancer (Auckl) 2015;9(Suppl 1):23.
7. Tobin NP, Foukakis T, De Petris L, et al. The importance of molecular markers for diagnosis and selection of targeted treatments in patients with cancer. J Intern Med 2015; 278:545.
8. Larson SM, Carrasquillo JA, Cheung NK, et al. Radioimmunotherapy of human tumours. Nat Rev Cancer 2015; 15:347.
9. Apostolidis C, Molinet R, Rasmussen G, et al. Production of Ac-225 from Th-229 for targeted alpha therapy. Anal Chem 2005;77:6288.
10. Dadachova E, Kitchen SG, Bristol G, et al. Casadevall preclinical evaluation of a ^{213}Bi-labeled 2556 antibody to HIV-1 gp41 glycoprotein in HIV1 mouse models as a reagent for HIV eradication. PLoS One 2012;7: e31866.
11. Yao Z, Garmestani K, Wong KJ, et al. Comparative cellular catabolism and retention of Astatine-, Bismuth-, and Lead-radiolabeled internalizing monoclonal antibody. J Nucl Med 2001;42:1538.
12. Singh M, Ramos I, Asafu-Adjei D, et al. Curcumin improves the therapeutic efficacy of Listeria(at)-Mage-b vaccine in correlation with improved T-cell responses in blood of a triple-negative breast cancer model 4T1. Cancer Med 2013;2:571.
13. Dinchuk JE, Focht RJ, Kelley JA, et al. Absence of post-translational aspartyl beta-hydroxylation of epidermal growth factor domains in mice leads to developmental defects and an increased incidence of intestinal neoplasia. J Biol Chem 2002;277:12970.
14. Lawton M, Tong M, Gundogan F, et al. Aspartyl-(asparaginyl) beta-hydroxylase, hypoxia-inducible factor-alpha and Notch cross-talk in regulating neuronal motility. Oxid Med Cell Longev 2010;3:347.
15. Silbermann E, Moskal P, Bowling N, et al. Role of aspartyl-(asparaginyl)-β-hydroxylase mediated notch signaling in cerebellar development and function. Behav Brain Funct 2010;6:68.
16. Gundogan F, Bedoya A, Gilligan J, et al. siRNA inhibition of aspartyl-asparaginyl sparaginyl tion of aspartyl-asparaginyl De Paepe MEch signaling, and fetal growth. Pathol Res Pract 2011;207:545.
17. Maeda T, Taguchi K, Aishima S, et al. Clinicopathological correlates of aspartyl (asparaginyl) beta-hydroxylase over-

expression in cholangiocarcinoma. Cancer Detect Prev 2004;28:313.
18. Gundogan F, Elwood G, Longato L, et al. Impaired placentation in fetal alcohol syndrome. Placenta 2008;29:148.
19. Sepe PS, Lahousse SA, Gemelli B, et al. Role of the aspartyl-asparaginyl-beta-hydroxylase gene in neuroblastoma cell motility. Lab Invest 2002;82:881.
20. Baklaushev VP, Grinenko NF, Yusubalieva GM, et al. Modeling and integral X-ray, optical, and MRI visualization of multiorgan metastases of orthotopic 4T1 breast carcinoma in BALB/c mice. Bull Exp Biol Med 2015;158: 581.
21. Zhang Y, Miwa S, Zhang N, et al. Tumor-targeting Salmonella typhimurium A1-R arrests growth of breast-cancer brainmetastasis. Oncotarget 2015;6:2615.
22. Yoshida T, Jin K, Song H, et al. Effective treatment of ductal carcinoma in situ with a HER-2- targeted alpha-particle emitting radionuclide in a preclinical model of human breast cancer. Oncotarget 2016;7:33306.
23. Li HK, Morokoshi Y, Daino K, et al. Transcriptomic signatures of auger electron radioimmunotherapy using nuclear targeting (111)In-trastuzumab for potential combination therapies. Cancer Biother Radiopharm 2015;30:349.
24. Razumienko EJ, Chen JC, Cai Z, et al. Dual-receptor-targeted radioimmunotherapy of human breast cancer xenografts in athymic mice coexpressing HER2 and EGFR using 177Lu- or 111In-labeled bispecific radioimmunoconjugates. J Nucl Med 2016;57:444.
25. Baidoo KE, Yong K, Brechbiel MW. Molecular pathways: Targeted α-particle radiation therapy. Clin Cancer Res 2013; 19:530.
26. Kratochwil C, Giesel FL, Bruchertseifer F, et al. 213Bi-DOTATOC receptor-targeted alpha-radionuclide therapy induces remission in neuroendocrine tumours refractory to beta radiation: A first-in-human experience. Eur J Nucl Med Mol Imaging 2014;41:2106.
27. Jurcic JG, Larson SM, Sgouros G, et al. Targeted alpha particle immunotherapy for myeloid leukemia. Blood 2002; 100:1233.
28. Allen BJ, Raja C, Rizvi S, et al. Intralesional targeted alpha therapy for metastatic melanoma. Cancer Biol Ther 2005;4: 1318.